HCl Uptake through Films of Pentanoic Acid and Pentanoic Acid/Hexanol Mixtures at the Surface of Sulfuric Acid

Daniel K. Burden, Alexis M. Johnson, and Gilbert M. Nathanson*

Department of Chemistry, University of Wisconsin—Madison, 1101 University Avenue, Madison, Wisconsin 53706-1322

Received: July 28, 2009; Revised Manuscript Received: October 16, 2009

Molecular beam scattering experiments are used to investigate collisions and reactions of HCl with deuterated sulfuric acid containing 0−0.2 M pentanoic acid (PA) and mixtures of PA and hexanol. Surface tension measurements at 296 K indicate that PA segregates to the surface of the acid, reaching coverages of 58% and 52% of maximum packing on 60 and 68 wt % D_2SO_4, respectively. We find that these films increase HCl entry into the acid at low PA surface coverage at 213 K. This enhancement is attributed to the dissociation of HCl molecules that come into contact with surface COOH groups and protonate them. At higher coverages, the PA film becomes more compact and impedes HCl uptake. Comparisons with films of pure hexanol and pentanoic acid/hexanol mixtures indicate that surface OH groups are more effective than COOH groups in catalyzing HCl entry. They also suggest that the PA films consist of patchy regions of tightly packed molecules, which are pushed away from the surface upon addition of the more surface active hexanol. HCl entry into the pure and mixed films can be analyzed quantitatively using a two-step model in which adsorbed HCl molecules penetrate between the alkyl chains and then dissociate at the surfactant−acid interface.

Introduction

Organic surfactants at the surface of aerosol particles can dramatically alter the rates of gas−liquid reactions, in part by impeding gas transport, changing the composition of the interface, or reacting directly with the gas molecule.[1−3] While organic molecules are plentiful in the lower troposphere,[4,5] recent field measurements indicate that aqueous aerosols in the upper troposphere and even lower stratosphere also contain organic matter.[6,7] Neither the abundance nor the nature of these organic species is firmly established, but they may be expected to range from small molecules such as methanol to long-chain carboxylic acids.[5,8] In the lower stratosphere, sulfuric acid droplets mediate the conversion of temporary reservoir species containing chlorine and bromine (HCl, HBr, HOCl, HOBr, $ClONO_2$, $BrONO_2$) into Cl_2, BrCl, and Br_2, which are then photolyzed by sunlight into radicals that catalytically destroy ozone.[9−11] These droplets also convert N_2O_5 into soluble HNO_3, thereby denitrifying the atmosphere and enhancing ozone depletion.[9−12] Surfactant coatings may be one explanation for the measured variability in N_2O_5 hydrolysis rates in aqueous aerosols over the northeast United States.[13] This hypothesis is supported by laboratory studies of soluble and insoluble monolayers on aqueous solutions, including sulfuric acid, which demonstrate that these films significantly impede the hydrolysis of N_2O_5,[14−18] evaporation of water and bromine,[19−21] and uptake of carbon dioxide, oxygen, ammonia, nitric acid, and acetic acid.[22−25]

Our own experiments indicate that the soluble surfactants butanol and hexanol form films on sulfuric acid that also impede N_2O_5 hydrolysis[26] while enhancing the entry of HCl and HBr.[3,27,28] In this study, we explore the effects of pentanoic acid and mixed pentanoic acid/hexanol films on HCl entry into 60 and 68 wt % D_2SO_4 at 213 K, which mimic conditions in the midlatitude tropopause region. Figure 1a depicts events that may occur when HCl molecules collide with a D_2SO_4 solution covered with a monolayer of pentanoic acid, $CH_3(CH_2)_3COOH$, based on our previous studies of bare and alcohol-coated D_2SO_4 solutions.[3] Impinging HCl molecules may recoil directly from the surface (inelastic scattering) or dissipate their excess kinetic energy and become momentarily trapped at the surface, losing memory of their initial trajectory. At thermal collision energies near $2RT_{liq} = 3.5$ kJ mol^{-1}, nearly all HCl molecules become trapped by attractive forces between the gas and surface species. Some of these thermalized molecules desorb (TD) from the top of the film or after moving between the surfactant chains and returning to the surface. The remaining HCl molecules also permeate through the film but dissociate at or near the surfactant−acid interface and dissolve in the acid as ions, emerging later as DCl.

To characterize these processes, we measure the fraction f_{exch} of thermalized HCl molecules that undergo H → D exchange in the deuterated acid and desorb as DCl. The average residence time of the unexchanged HCl molecules is less than 10^{-6} s, our shortest measurable time, implying that these species thermalize on the surface and immediately desorb.[27,29] We find that HCl molecules that undergo H → D exchange have average residence times ranging from 10^{-4} s in 70 wt % D_2SO_4 to 10^{-2} s in 56 wt % D_2SO_4. These times correspond to diffusion depths of 10^2 to 10^3 Å in the acid.[30,31] The sharp difference in residence times for unexchanged HCl and H → D exchanged DCl imply that f_{exch} is equal to the fraction of thermalized HCl molecules that enter the acid, either as molecular HCl or as Cl^- and H^+ after dissociating first in the interfacial region.[32] For uncoated acid solutions, f_{exch} rises with increasing dilution, most likely because more D_2O molecules in the surface region act as hydrogen bonding and dissociation sites for adsorbed HCl.[22,33]

The addition of butanol or hexanol to sulfuric acid significantly alters HCl entry.[27,28] Both alcohols segregate to the surface of the acid, forming an outer layer of ROD and ROD_2^+ and small amounts of $ROSO_3D$ and $ROSO_3^-$.[34] This segregation generates a surface film that contains both alkyl chains and OD

* Corresponding author, nathanson@chem.wisc.edu.

10.1021/jp9072119
Published on Web 11/19/2009

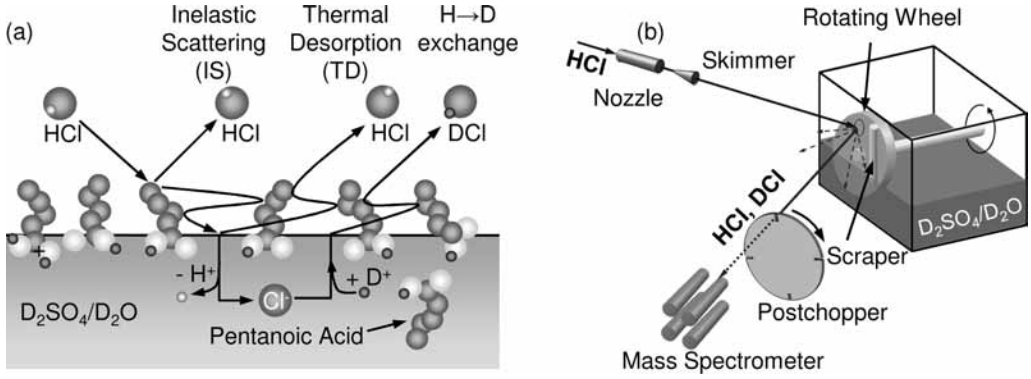

Figure 1. (a) Observed pathways for an HCl molecule colliding with deuterated sulfuric acid that is partly covered with pentanoic acid molecules. (b) Schematic diagram of the scattering apparatus.

TABLE 1: Properties of Pure and Surfactant-Doped Sulfuric Acid Solutions

property	temperature (K)	D_2SO_4 concentration (wt %) 59.5	67.5
pure sulfuric acid			
D_2SO_4 mole fraction		0.227	0.293
equivalent H_2SO_4 concentration (wt %)		61.5	69.3
viscosity (cP)[a]	213	470	1800
H_2O vapor pressure (Torr)[b]	213	9.4×10^{-4}	2.4×10^{-4}
H^+ activity (mole fraction scale)[b]	213	200	2000
bulk-phase surfactant protonation[c]			
estimated mole fraction $C_4H_9COOD_2^+$	310	~0.13	~0.23
estimated mole fraction $C_6H_{13}OD_2^+$	295	~0.25	~0.35
estimated basicity C_4H_9COOH (pK_{BH^+})[d]	310	−2.8	
estimated basicity $C_6H_{13}OH$ (pK_{BH^+})[d]	295	−2.0	
pentanoic acid (PA) surface properties	296		
asymptotic surface coverage c_∞(10^{14} cm^{-2})		~2.9	~2.6
fraction of compact monolayer		~58%	~52%
Langmuir constant K_L (M^{-1})		96 ± 6	84 ± 4
hexanol surface properties	296		
asymptotic surface coverage c_∞(10^{14} cm^{-2})		~3.0	~2.7
fraction of compact monolayer		~60%	~54%
Langmuir constant K_L (M^{-1})		410 ± 10	360 ± 10
HCl entry model (eq 6)[e]	213		
PA blocking parameter *a*		1.27 ± 0.02	1.11 ± 0.02
hexanol blocking parameter *a*		1.05 ± 0.01	0.8 ± 0.1
PA headgroup protonation constant *b*		0.95 ± 0.04	0.15 ± 0.01
hexanol headgroup protonation constant *b*		1.34 ± 0.02	0.36 ± 0.06

[a] Calculated from refs 35 and 36. [b] Calculated from ref 37. [c] Calculated from refs 38 and 39 for 3-methylbutanoic acid and 1-propanol. [d] K_{BH^+} is the equilibrium constant for $BH^+ \rightleftharpoons B + H^+$. It was reevaluated using the excess acidity method (ref 66) with data from refs 38, 39, and 67 for 2-butanoic acid and 1-propanol. The ratio $K_{BH^+}(COOH)/K_{BH^+}(OH)$ is ~6.3. [e] The error bars represent ±1 standard deviation of the least-squares fit of eq 6 to Figure 8a,b.

groups from the alcohol, leading to two competing effects: the alkyl chains may pack tightly enough to impede transport, while the OD groups provide additional interfacial sites for the dissociation of HCl molecules that reach the acid. We find that surface butanol molecules always enhance HCl entry, perhaps because these short chains cannot pack tightly enough to impede entry. Hexanol, while also facilitating HCl entry at low coverages, imposes a barrier at higher coverage as the longer chains pack more tightly.

Are alcohols the only surfactants that enhance HCl entry? In this study, we substitute COOH for OH and explore the basicity and packing of pentanoic acid (PA), the lowest melting carboxylic acid. The experiments reveal that PA molecules also enhance HCl entry, but only at low coverage, and that they are replaced at the surface by even small additions of hexanol.

Properties of Pentanoic Acid and Hexanol in Supercooled Sulfuric Acid

Table 1 lists properties of 59.5 and 67.5 wt % D_2SO_4 and the surfactants used in the experiments. The viscous acid solutions have vapor pressures below 10^{-3} Torr at 213 K.[35−37] D_2SO_4 dissociates in both solutions, forming mixtures of D_2O, D_3O^+, DSO_4^-, and SO_4^{2-}.[37] PA and hexanol dissolve in 68 wt % D_2SO_4 at concentrations up to 0.2 M without freezing at 213 K, even though this temperature is 12 and 26 K below the melting points of the alcohol and carboxylic acid, respectively. As noted later, PA does freeze in 60 wt % D_2SO_4 at concentrations above 0.1 M. Each surfactant undergoes protonation in sulfuric acid: NMR studies of 3-methylbutanoic acid[38] and 1-propanol[39] indicate that the carboxylic acid ($pK_{BH^+} = -2.8$) is ~13% protonated in 59 wt % H_2SO_4 and ~23% protonated in 69 wt % acid at 310 K, while the more basic alcohol ($pK_{BH^+} = -2.0$) is ~25% and ~35% protonated in these solutions at 273 K. Literature data suggest that these fractions increase only slightly at 213 K.[40] Hexanol may also form hexylsulfuric acid, $C_6H_{13}OSO_3D$, but this reaction is slow even at room temperature.[41] We estimate that less than 2% of the alcohol is converted to this acid during our experiments, and we ignore it in the analysis below. The ester hexyl pentanoate, $C_6H_{13}COOC_4H_9$, may also form in mixtures of PA and hexanol in sulfuric acid.

We could observe weak evaporation attributable to the ester at 213 K in some experiments at high surfactant concentrations, but surface tension measurements at 296 K shown later in Figure 6 do not provide evidence for a third surface-active component.

Experimental Procedure

All sulfuric acid solutions are prepared by diluting 98 wt % D_2SO_4 with D_2O and then placing 60 mL of the solution into the Teflon reservoir pictured in Figure 1b. PA and hexanol are added to the acid at ~280 K by dropping them onto the surface with a micropipet. All reagents were used as purchased (Sigma-Aldrich). PA and hexanol are fully converted into their COOD and OD analogues, which reduce the deuterium fraction of the acid by less than 0.3%.

As depicted in Figure 1b, a continuously renewed, vertical liquid film is formed by rotating a 5 cm diameter glass wheel partially submerged in the acid mixture at 213 K.[42] The coated wheel is skimmed by a Teflon scraper, which leaves behind a ~0.5 mm thick acid film. The scraped film then passes in front of a 0.7 cm^2 hole in the reservoir, where it is exposed to Ar or HCl for 0.27 s at a typical wheel speed of 0.17 Hz. The time between scraping and exposure to the incident beam is 0.49 s, which is sufficient to reestablish the surfactant molecules at the surface of the acid.[42] Solutions containing hexanol at 0.1−0.2 M form a thick coating of small bubbles, which are wiped away by the scraper. Ar scattering measurements shown later do not reveal any abrupt changes at the onset of bubble formation.

Incident beams of Ar (90 kJ mol^{-1}) and HCl (10 and 100 kJ mol^{-1}) are directed at the surface of the acid at an incident angle of 45°, projecting a 0.36 × 0.51 cm^2 beam spot. The exiting Ar, HCl, and DCl species are then chopped into 40 μs pulses using the postchopper wheel depicted in Figure 1b and are detected by a mass spectrometer at an exit angle of 45°. Their arrival times at the mass spectrometer are measured over a 19 cm flight path and displayed as time-of-flight (TOF) spectra.

Results and Analysis

Surface Tensions and Surface Concentrations. Measurements of the surface tension σ can be used to determine the approximate relative surface excess Γ^{PA} of pentanoic acid species (C_4H_9COOH and $C_4H_9C(OH)_2^+$) or Γ^{hex} of hexanol species ($C_6H_{13}OH$ and $C_6H_{13}OH_2^+$) with respect to zero excess of H_2O in sulfuric acid.[34,43,44] The measurements were made with H_2SO_4 solutions at 296 K using the Wilhelmy method and a 1.03 mm diameter Pt pin. With PA as an example, the surface excess is calculated from the Gibbs adsorption equation[43]

$$\Gamma^{PA} = \Gamma^{C_4H_9COOH} + \Gamma^{C_4H_9C(OH)_2^+} \approx \frac{-c_{bulk}^{PA}}{RT}\left(\frac{\partial\sigma}{\partial c_{bulk}^{PA}}\right)_T \quad (1)$$

where c_{bulk}^{PA} is the formal bulk-phase concentration of PA.[45] This relation is likely to be accurate to only ~10% because the acid is a multicomponent solution whose chemical potentials may vary upon addition of PA, while only the temperature is held constant experimentally.[34] Under conditions where C_4H_9COOH and $C_4H_9C(OH)_2^+$ segregate solely in a monolayer at the surface, the relative excess Γ^{PA} can be related to the absolute number of surfactant species per unit area at the surface, $c_{surf}^{PA} = c_{surf}^{C_4H_9COOH} + c_{surf}^{C_4H_9C(OH)_2^+}$, according to[43]

$$\Gamma^{PA} = c_{surf}^{PA} - c_{surf}^{H_2O}\frac{x_{bulk}^{PA}}{x_{bulk}^{H_2O}} \approx c_{surf}^{PA} \quad (2)$$

where $c_{surf}^{H_2O}$ is the surface concentration of H_2O molecules and x_{bulk} is the bulk-phase mole fraction of PA or water. The ratio of these mole fractions never exceeds 0.01 in our experiments. In this case, the relative surface excess $\Gamma^{PA}$and the absolute surface concentration c_{surf}^{PA} differ by less than 1%, and we set them equal to each other in the analysis below.[46] Analogously, Γ^{hex} and $c_{surf}^{hex} = c_{surf}^{C_4H_9OH} + c_{surf}^{C_6H_{13}OH_2^+}$ are also assumed to be equal.[34]

Panels a and b of Figure 2 show the changes in surface tension upon addition of PA and hexanol in 61 and 69 wt % H_2SO_4 at 296 K. σ(hexanol) drops more sharply than σ(PA), indicative of a steeper rise in the hexanol surface excess, as shown in panels c and d. The lines in panels a−d are fits to the Langmuir adsorption isotherm for c_{surf}^{PA} or c_{surf}^{hex}

$$c_{surf} = c_\infty\frac{K_L c_{bulk}}{(1 + K_L c_{bulk})} \quad (3)$$

where c_∞ is the asymptotic surface concentration of PA or hexanol species and K_L is a measure of the propensity for segregation, such that $1/K_L$ is equal to the concentration where $c_{surf} = (1/2)c_\infty$.[47] The values of K_L and c_∞ for PA and hexanol are listed in Table 1. As expected from the shapes of the surface excess curves, K_L is smaller for PA (which saturates near 0.1 M) than for hexanol (which saturates near 0.05 M).

The fits in Figure 2 indicate that c_∞ reaches values of 2.6 and 2.7 × 10^{14} cm^{-2} for PA and hexanol, respectively, in 69 wt % H_2SO_4 at 296 K. They correspond to surface coverages of alkyl chains of ~52% and ~54% of a compact, all-trans alkane monolayer based on a maximum packing of ~5 × 10^{14} cm^{-2}.[1,48−51] The surface concentrations rise slightly in 61 wt % H_2SO_4 to 2.9 and 3.0 × 10^{14} cm^{-2} for PA and hexanol, corresponding to ~58% and ~60% of a compact monolayer. These higher coverages likely occur because fewer OH and COOH groups are protonated at lower acid concentrations, making them less soluble in the bulk and reducing charge repulsion between the headgroups at the surface.[52]

Hyperthermal Argon Scattering from Pentanoic Acid Films on Sulfuric Acid. Inert gas scattering can be used to detect surfactant molecules at the surface of the acid because of the change in mass and roughness that occur upon segregation of the alkyl chains.[42] Figure 3a shows TOF spectra of the scattering of argon atoms from solutions of 0−0.2 M PA in 60 wt % D_2SO_4 at 213 K. The incident energy E_{inc} is 90 kJ mol^{-1} ($51RT_{liq}$). The sharp peak at early arrival times corresponds to Ar atoms that scatter from the liquid after one or a few collisions. These atoms recoil on average with ~30% of their incident energy in this inelastic scattering (IS) channel. The broader peak at later arrival times corresponds to Ar atoms that dissipate their excess kinetic energy and then thermally desorb (TD). This TD component is fit well by a Maxwell−Boltzmann distribution at the temperature of the acid (not shown).

Figure 3a demonstrates that the addition of PA significantly alters collisions of Ar atoms. As the PA concentration is increased to 0.2 M, the TD signal grows and the IS signal shrinks and shifts to later arrival times. These changes reflect the greater energy loss suffered by Ar atoms colliding with alkyl chains than with bare sulfuric acid. The shift in arrival times (dashed arrow in panel a) may be used to calculate the average

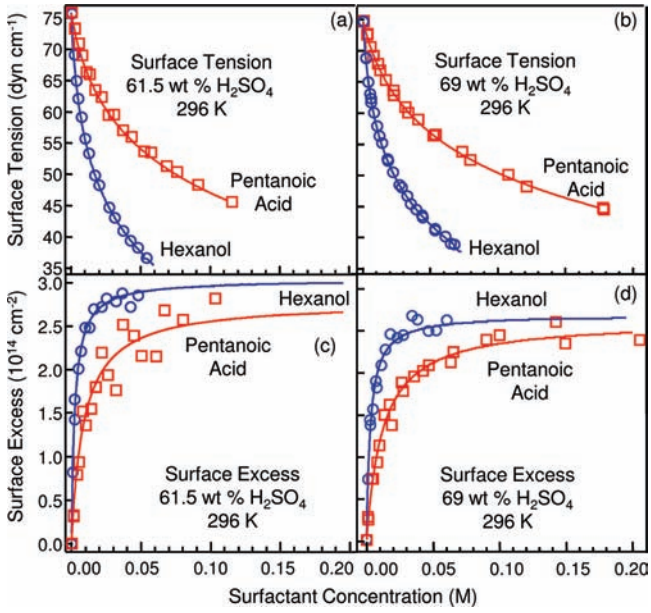

Figure 2. Surface tension of pentanoic acid− and hexanol−sulfuric acid mixtures at 296 K in (a) 61 wt % H_2SO_4 and (b) 69 wt % H_2SO_4. (c, d) Gibbs surface excesses obtained from eq 1 and the surface tensions. The solid lines are fits to a Langmuir adsorption isotherm with asymptotic concentrations c_∞ and Langmuir constants K_L listed in Table 1.

energy lost by Ar atoms in the IS channel, equal to $[E_{inc} - \langle E_{IS}\rangle]/E_{inc}$. These are shown as solid symbols in panels b and c, while the open symbols refer to the PA surface concentration from Figure 2c,d. The two sets approximately overlap, as they do for butanol and hexanol,[28,42] suggesting that the vertical surfactant films created in vacuum at 213 K mimic those prepared horizontally at 296 K on the benchtop.

Collisions of HCl with Pentanoic Acid Films on Sulfuric Acid. We next use H → D exchange measurements to explore the effects of surface PA molecules on HCl entry into the acid. Figure 4a shows HCl and DCl TOF spectra following collisions of 100 kJ mol^{-1} HCl with an uncoated 60 wt % D_2SO_4 solution at 213 K. This figure illustrates the three channels depicted in Figure 1a: inelastic scattering of HCl, thermal desorption of intact HCl, and thermal desorption of H → D exchanged DCl. The intensities of the thermally desorbing DCl and HCl molecules, I_{TD}, can then be used to determine the H → D exchange fraction f_{exch}[29]

$$f_{exch} = \frac{I_{TD}^{DCl}}{I_{TD}^{DCl} + I_{TD}^{HCl}} \quad (4)$$

Figure 4a indicates that 46% of the thermally desorbing molecules have undergone H → D exchange and emerge as DCl. Panel b further shows that f_{exch} drops to 0.36 upon adding PA to reach 0.05 M. At this molarity, the PA surface concentration is ~2.3 × 10^{14} cm^{-2} at 296 K, equal to nearly 50% of maximum packing.

As stated in the Introduction, we interpret f_{exch} to be the fraction of thermalized HCl molecules that enter the acid as Cl^- and H^+ ions after dissociating in the surface region or that enter intact and then dissociate into Cl^- and H^+ below the surface. This interpretation is based on two observations.[29] First, pulsed-beam experiments show that the average time between HCl entry and DCl desorption is 130 μs in 60 wt % D_2SO_4 at

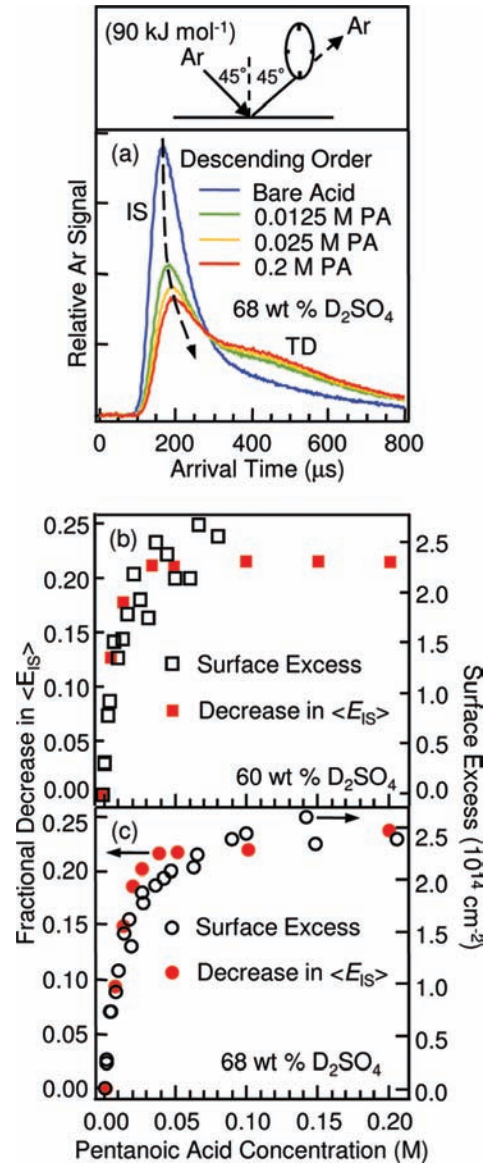

Figure 3. (a) Time of flight (TOF) spectra of 90 kJ mol^{-1} Ar atoms scattering from pentanoic acid−sulfuric acid mixtures at 213 K. (b) and (c) Solid red symbols: fractional decrease in energy of inelastically scattered Ar atoms, plotted on the left axis. Open black symbols: pentanoic acid surface excess at 296 K from parts c and d of Figure 2, plotted on the right axis.

213 K, a delay time which is attributed to diffusion of the HCl/Cl^-/DCl species into the acid.[27] Because this bulk-phase residence time is much shorter than the 0.27 s exposure time of the acid to the incident HCl beam, nearly all (~99%) dissolved Cl^- ions recombine and leave as DCl during the 0.27 s interval.[53] In this case, almost all HCl molecules that enter the acid are accounted for as DCl molecules that desorb from the acid. Second, previous studies indicate that the HCl trapping (thermalization) probability approaches 1 as the incident energy is lowered to values near $2RT_{liq}$, while f_{exch} itself remains constant.[27,29] These statements imply that HCl entry is a two-step process in which the HCl molecules are first trapped on the surface and then dissociate (and later desorb as DCl), such that $p_{enter} = p_{trap}f_{exch}$. We tested this conjecture again here by lowering the collision energy from 100 to 10 kJ mol^{-1}, as shown in Figure 4c,d for bare and 0.05 M PA−60 wt % D_2SO_4. Nearly all incoming HCl molecules thermalize at this low energy. The measured f_{exch} values are 0.47 and 0.39 for bare and 0.05 M

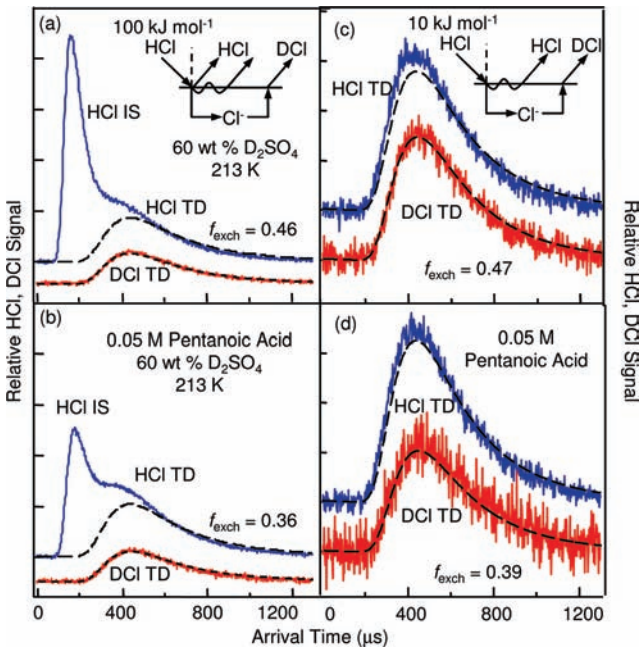

Figure 4. TOF spectra of (a) HCl and (b) H → D exchanged DCl following collisions of HCl at $E_{inc} = 100$ kJ mol^{-1} with 60 wt % D_2SO_4 at $T_{liq} = 213$ K. Same for (c) and (d) at $E_{inc} = 10$ kJ/mol. The thermal desorption (TD) component peaks are fit well by a Maxwell−Boltzmann distribution (dotted curves) at T_{liq}.

PA, equal to the 0.46 and 0.36 values at $E_{inc} = 100$ kJ mol^{-1} within experimental uncertainty. These experiments reaffirm that f_{exch} equals p_{enter} under thermal collision conditions as p_{trap} approaches 1.

Panels a and b of Figure 5 summarize the f_{exch} measurements for 60 and 68 wt % D_2SO_4 at PA concentrations up to 0.2 M. The error bars represent ±1 standard deviation for two to nine measurements: for the bare acid, $\langle f_{exch} \rangle = 0.464 \pm 0.011$ (60 wt % D_2SO_4) and 0.083 ± 0.002 (68 wt % D_2SO_4).[54] Panel a shows that f_{exch} (solid circles) first rises with the addition of PA at 0.006 M and then drops below the bare acid value as the PA surface concentration (open circles) increases. The measurements fluctuate beyond ~0.1 M because pentanoic acid begins to freeze (◇ symbols). The trend is clearer in 68 wt % D_2SO_4 in panel b, where freezing did not occur. The H → D exchange fraction starts at 0.083 for the bare acid, rises to 0.088, and then drops smoothly and steadily below the bare acid value to 0.07 at high PA surface coverage.

To place the PA results in perspective, Figure 5c,d shows the changes brought about by hexanol films on 60 and 68 wt % acid. These values were reported earlier[28] and remeasured here. They show that f_{exch} rises and then turns over when adding hexanol to 60 wt % D_2SO_4 but does not drop below the bare acid value. For 68 wt % acid, f_{exch} rises sharply upon adding hexanol, with no evidence for a turnover. The cumulative data in Figure 5 indicate that PA increases HCl entry at low coverages, suggesting that the COOH headgroup, like OH, can act as an interfacial dissociation site for an acidic gas molecule. This enhancement is never as great as that for hexanol, and the PA molecules eventually impede HCl entry at high PA surface coverages, implying that the competition between headgroup protonation and chain packing is different for PA and hexanol. This competition is quantified in the Discussion.

Surface Tension and Ar Scattering Studies of Hexanol and Pentanoic Acid Mixtures in 68 wt % D_2SO_4. The comparisons of hexanol and pentanoic acid in Figure 5 prompted us to ask how mixtures of the two surfactants would alter HCl entry into

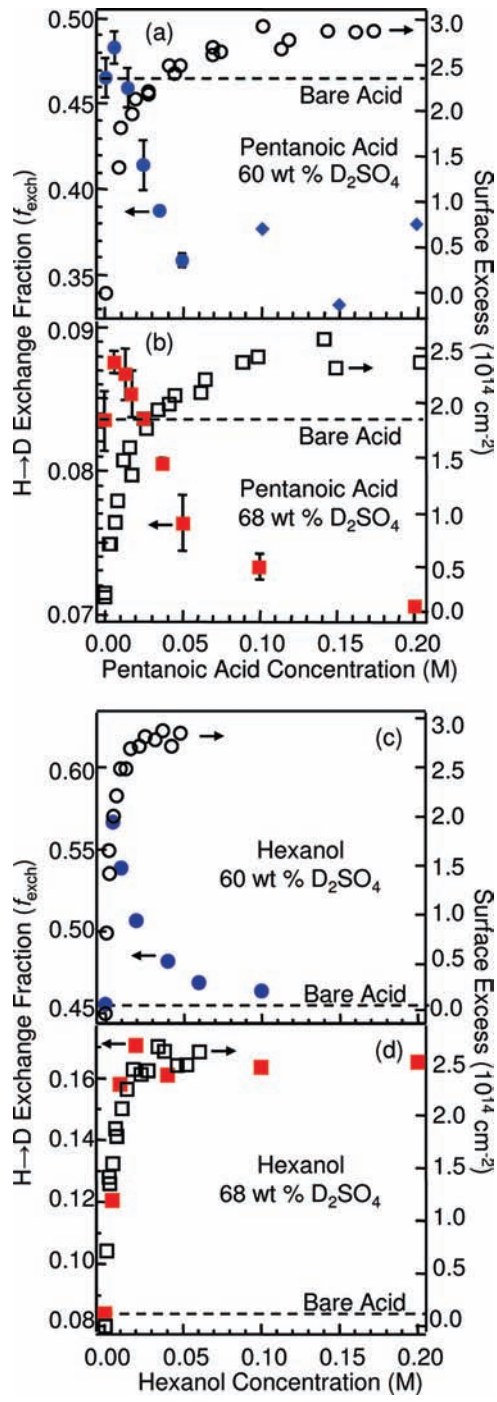

Figure 5. HCl → DCl exchange fraction f_{exch} versus pentanoic acid concentration in (a) 60 and (b) 68 wt % D_2SO_4 and versus hexanol concentration in (c) 60 and (d) 68 wt % acid. The surface excess values are plotted on the right axis in each panel, obtained from Figure 2.

the acid. Studies by Bertram and Vaida and co-workers, for example, show that the addition of a branched or bent surfactant into straight-chain alcohol monolayers reduces the resistance of the film to uptake of N_2O_5 and acetic acid, while earlier studies indicate that the resistance to water evaporation may be reduced (at high surface pressure) or enhanced (at lower surface pressure) by adding a shorter surfactant to the alcohol monolayer.[17,23,55] Gas−surfactant reactions, such as the ozonolysis of fatty acids, may even alter the composition of mixed films by preferentially reacting with one of the components, as recently demonstrated by Allen and co-workers.[56] To explore the effects of mixed surfactants on HCl entry, we prepared

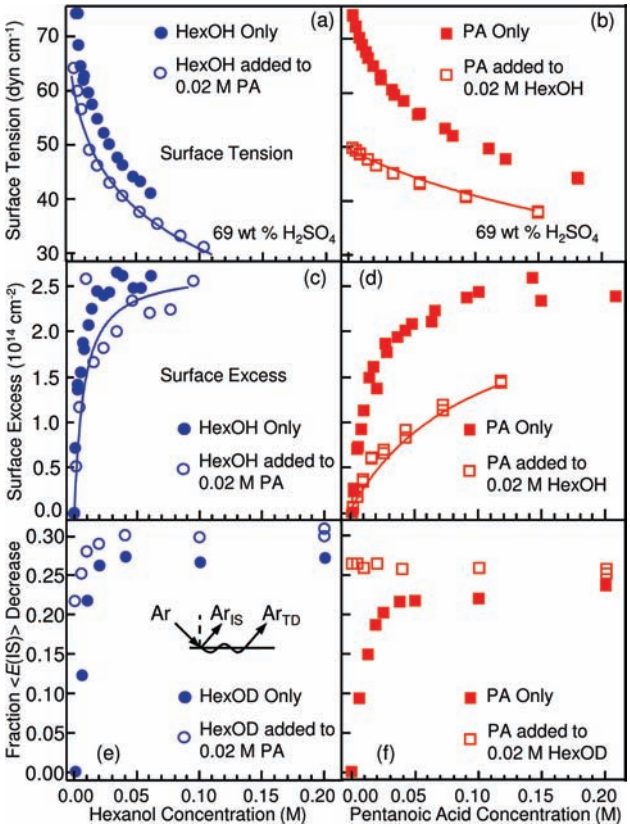

Figure 6. (a) Surface tensions of 69 wt % H_2SO_4 at 296 K containing only hexanol (●) and 0.02 M pentanoic acid mixed with hexanol (○). (b) Same for the 69 wt % H_2SO_4 containing only pentanoic acid (■) and 0.02 M hexanol mixed with pentanoic acid (□). (c) and (d) Gibbs surface excess values calculated from eq 1 and the surface tension measurements. The solid lines are fits to eq 5. (e and f) Argon atom scattering from the mixtures at 213 K, where $[E_{inc} - \langle E_{IS}\rangle]/E_{inc}$ is plotted against surfactant concentration at 296 K.

mixtures in 68 wt % D_2SO_4 by adding PA to 0.02 M hexanol and adding hexanol to 0.02 M PA. Figure 2 shows that, at 296 K, the initial surface concentrations are 2.4×10^{14} cm^{-2} (48% of maximum packing) for 0.02 M hexanol and 1.6×10^{14} cm^{-2} (32% of maximum packing) for 0.02 M PA.

Figure 6 compares surface tension and Ar scattering measurements of the mixtures with hexanol and PA individually. Panels a and b reveal that the drop in surface tension is shallower for the mixtures than for pure PA and pure hexanol. The surface excesses in panel c and d are calculated using eq 1 at constant bulk concentration of one surfactant.[57,58] Panel c shows that the surface excess of hexanol alone is initially larger than when hexanol is added to a 0.02 M PA solution in 68 wt % D_2SO_4. However, the surface excesses converge at higher concentrations, implying that pentanoic acid has been mostly replaced by hexanol. In panel d, the surface excess of PA is much less in the 0.02 M hexanol solution than when PA is added to the pure acid, and it does not reach the same coverage even at 0.12 M PA in 0.02 M hexanol. These surface excesses, equal to the partial surface concentrations c_{surf}^{PA} and c_{surf}^{hex}, can be modeled using a two-component Langmuir adsorption isotherm, given by[47]

$$c_{surf}^{PA} = c_{\infty}^{PA}\frac{K_L^{PA}c_{bulk}^{PA}}{(1 + K_L^{PA}c_{bulk}^{PA} + K_L^{hex}c_{bulk}^{hex})} \quad (5)$$

with an analogous expression for hexanol. The solid lines in panels c and d are fits to c_{surf}^{hex} and c_{surf}^{PA}, respectively, along with

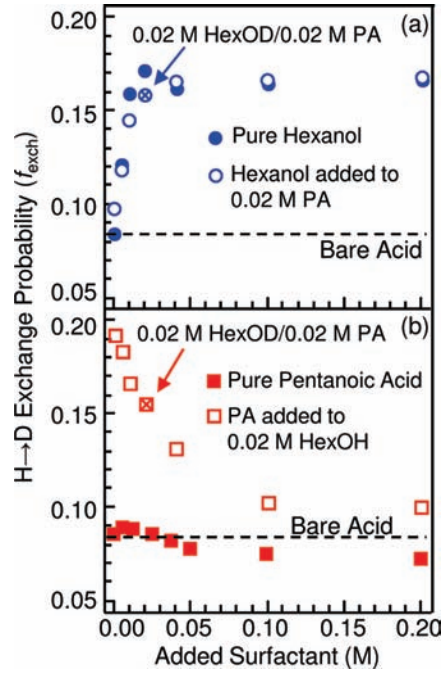

Figure 7. H → D exchange fraction f_{exch} (a) for 68 wt % D_2SO_4 containing only hexanol (●) and 0.02 M pentanoic acid mixed with hexanol (○) and (b) for 68 wt % D_2SO_4 containing only pentanoic acid (■) and 0.02 M hexanol mixed with pentanoic acid (□).

corresponding fits to the surface tensions in panels a and b. As discussed later, the good fits imply that the PA and hexanol molecules interact at most weakly at the surface, indicative either of ideal mixing or of lateral segregation into separate domains.

The Ar scattering measurements reveal a slightly different picture because Ar atoms lose energy upon collision with both PA and hexanol molecules at the surface. Panel e shows that the fraction of energy lost by the Ar atoms is nearly the same for the hexanol + 0.02 M PA mixture and for hexanol alone, with differences that lie within the reproducibility of the measurements. The energy transfer initially rises as hexanol is added to the mixture, indicating that hexyl chains can insert at the surface of a 0.02 M PA film, just as inferred from the surface excess curve in panel c. This is not the case when PA is added to 0.02 M hexanol. The Ar energy transfer changes very little, implying that the overall chain density remains roughly constant as PA replaces a surface initially covered with hexanol.

Collisions of HCl with Pentanoic Acid/Hexanol Mixtures on Sulfuric Acid. The greater surface activity of hexanol is readily apparent in measurements of HCl entry into the mixture. Figure 7a shows that f_{exch} is nearly identical for films of pure hexanol and hexanol added to 0.02 M PA, again implying that hexanol readily displaces PA at the surface. In contrast, when PA is added to 0.02 M hexanol (panel b), f_{exch} slowly drops toward pure PA values as PA replaces hexanol at the surface, although it does not resemble pure PA even when its concentration is 10 times greater than that of hexanol. The reproducibility of the exchange measurements can be checked when each surfactant is at 0.02 M, as indicated by the arrows; f_{exch} is found to differ by less than 0.01. A quantitative analysis of the trends in Figure 7 is given below.

Discussion

The measurements of H → D exchange in Figure 5a,b suggest that PA films can enhance HCl entry at low surface coverages while impeding gas transport at high coverages. For hexanol in

60 wt % D_2SO_4 in Figure 5c, the rise and fall in f_{exch} was rationalized by arguing that, at low coverages where the monolayer is porous, the interfacial alcohol molecules provide additional OD sites for HCl dissociation.[28] These sites become increasingly unreachable as the hexyl chains pack more tightly but not enough to lower HCl entry below the bare acid value. On 68 wt % acid, the OD headgroups are sufficiently protonated that charge repulsion limits chain−chain packing and HCl entry is enhanced by the availability of the unprotonated OD groups. In the sections below, we compare PA and hexanol quantitatively to unravel differences in headgroup protonation and chain packing and to understand how the surfactants mix at the surface.

Headgroup Protonation versus Chain Packing in Pure Pentanoic Acid and Hexanol Films. Figure 5 shows that surface PA molecules do not enhance HCl entry as effectively as hexanol molecules at low coverage and are more effective in blocking HCl entry at high coverage. Do these differences arise because PA packs more tightly than hexanol or because the OH groups of hexanol provide more facile protonation sites for HCl dissociation? To address this question, we use a crude model of HCl entry that distinguishes these possibilities. We assume that the surfactant molecules uniformly cover the surface of the acid and that gas entry occurs in two steps: (1) adsorbed HCl molecules move between the alkyl chains via sequential collisions and (2) HCl then dissociates at the headgroup−acid interface upon protonation of D_2O, PA, or hexanol. The probability for HCl entry, given by f_{exch}, would then be equal to the product of probabilities for HCl transport through the chains, $p_{transport}$, and for reaction with the surfactant headgroup or D_2O, $p_{dissociate}$, such that

$$f_{exch}(\text{surfactant}) = p_{transport}p_{dissociate} = \left[1 - a\frac{c_{surf}}{c_{max}}\right]\left[f_{exch}(\text{bare}) + b\frac{c_{surf}}{c_{max}}\right] \quad (6)$$

where c_{surf} is the surface concentration of surfactant and c_{max} is the maximum density of the alkyl chains themselves, set equal to 5×10^{14} cm^{-2} for both PA and hexanol.[50] In this model, the ease of HCl transport through the film, $p_{transport} = 1 - ac_{surf}/c_{max}$, is assumed to decrease with the surface concentration of surfactant, weighted by a constant $a \geq 0$ that measures the efficacy of PA or hexanol molecules to block transport of HCl. The value $a = 0$ implies that the monolayer is fully porous and does not hinder transport. Similarly, the dissociation probability, $p_{dissociate} = f_{exch}(\text{bare}) + bc_{surf}/c_{max}$, is assumed to increase with the surface concentration of ROD or RCOOD headgroups, where the constant $b \geq 0$ measures the ability of the headgroup to act as an extra hydrogen bonding and dissociation site for HCl. Within this model, $b = 0$ implies that the headgroups do not enhance HCl dissociation or interfere with the ability of the acid to capture HCl.[59]

The linear variations in eq 6 were chosen empirically as the simplest fit to the data. Similar linear trends have been observed in the suppression of HNO_3, NH_3, and N_2O_5 hydrolysis using butanol and hexanol monolayers on water and sulfuric acid.[22,26] These linear variations, however, cannot likely be extended to compact densities where c_{surf} closely approaches c_{max}. In this region, there is little free volume and chain motion is restricted. This case applies to long-chain insoluble surfactants spread on water, where $p_{transport}$ is found to decrease exponentially with increasing c_{surf}.[19] For short-chain soluble surfactants, the surface density is lower and it is not useful to think of c_{surf}/c_{max} as the fraction of occupied, impenetrable sites. The PA and hexanol molecules take up space at the surface but do not necessarily block HCl permeation because the chains are constantly in motion, and their fluctuating orientations and positions open gaps through which HCl molecules may move, although more tortuously as c_{surf} increases and the chains pack more tightly.[3,60] Equation 6 is a crude representation of HCl transport and reaction, but it is a function of only two variables, allowing trends in f_{exch} to be decomposed into a chain-blocking constant a and a headgroup reactivity constant b.

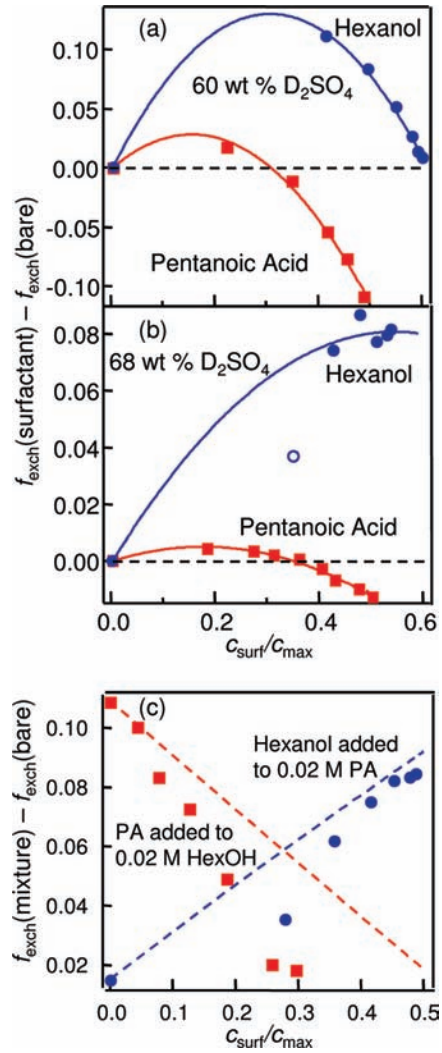

Figure 8. f_{exch} plotted against the dimensionless surface concentration c_{surf}/c_{max} of PA (red) or hexanol (blue) for (a) 60 and (b) 68 wt % D_2SO_4 at 213 K. The solid lines are fits to eq 6. The ordinate is the change in f_{exch}, set equal to f_{exch}(surfactant) − f_{exch}(bare). The open circle in panel b was not used in the hexanol fit because its inclusion predicts a chain block constant $a < 0$. (c) Changes in f_{exch} for the surfactant mixtures in 68 wt % D_2SO_4 against the partial surface concentration c_{surf}/c_{max} of PA (red) or hexanol (blue). The dashed lines are fits to eq 7a.

We use the surface concentrations in Figure 2 at 296 K for c_{surf} and plot f_{exch}(surfactant) − f_{exch}(bare) against c_{surf}/c_{max} for PA and hexanol in 60 and 68 wt % D_2SO_4 in Figure 8a,b. The two panels show clearly that, at each surface concentration, the PA film more effectively blocks HCl entry or enhances it less than the hexanol film. The solid line fits to eq 6 quantify this observation. For 60 wt % D_2SO_4, we find that the hexanol OH group ($b = 1.34 \pm 0.02$) is more effective than the pentanoic COOH group ($b = 0.95 \pm 0.04$) in enhancing HCl entry. This trend is expected because the hydroxyl group is more basic than

the carboxylic acid group, as indicated in Table 1 and is therefore more readily protonated by HCl. For 68 wt % acid, the b values are 0.36 ± 0.06 for hexanol and 0.15 ± 0.01 for PA. The smaller b values for 68 wt % than for 60 wt % acid likely reflect the smaller fraction of unprotonated OD and COOD headgroups at the surface of the more concentrated acid.

The fits in Figure 8 further indicate that PA molecules (a = 1.27 ± 0.02) block HCl entry more effectively than do hexanol molecules (a = 1.05 ± 0.01) for 60 wt % D_2SO_4. The same trends are found for the 68 wt % acid, where a = 1.11 ± 0.02 for PA and 0.8 ± 0.1 for hexanol. The greater blocking effect for PA is surprising because the four-carbon chain of PA is shorter than the six-carbon chain of hexanol and because the surface propensities K_L and asymptotic surface concentrations c_∞ are greater for hexanol than for PA at 296 K. Preliminary surface tension measurements indicate that these trends extend to 250 K as well. The Ar scattering measurements in Figure 2e,f further suggest that hexanol is at least as surface active as PA at 213 K, making it unlikely that PA forms a uniformly denser film than hexanol at this low temperature.

The greater blocking imposed by PA could arise from different structures of the PA and hexanol films. In particular, some PA molecules may cluster into impermeable patches on the acid surface at 213 K. These dense PA regions may be persistent macroscopic domains, signaling a two-phase liquid−solid coexistence region,[61,62] or they may involve only a few molecules, connected to each other in linear or cyclic arrangements through CO···OH hydrogen bonds between neighboring COOH groups.[63] Hexanol molecules might also cluster into dense regions,[64] but this process will be impeded by their greater protonation in sulfuric acid. Empirically, hexanol also seems less likely to form patchy regions because its melting point is 14 K lower than the 239 K melting point of PA. We initially thought that this domain formation could be investigated by monitoring HCl entry through mixtures of PA and hexanol; as described below, this attempt was unsuccessful, but it does suggest that eq 6 can be used to predict entry through two-component films.

Mixtures of Pentanoic Acid and Hexanol. Figure 7a indicates that HCl entry into 68 wt % D_2SO_4 is nearly identical for films of pure hexanol and hexanol mixed with 0.02 M PA. In contrast, panel b shows that mixtures of PA in 0.02 M hexanol do not behave like pure PA films even when the PA concentration is 10 times higher than that of hexanol. These results indicate that PA is less surface active than hexanol, echoing the single surfactant data in Figure 2. To separate this competitive adsorption from the effects of surface PA and hexanol molecules on HCl entry itself, we graph changes in f_{exch} against the *surface* concentration of PA and hexanol, c_{surf}/c_{max}, obtained from Figure 6c,d. The data are plotted as f_{exch}(mixture) − f_{exch}(bare) in Figure 8c. This graph shows that, with nearly equal propensity, hexanol enhances HCl entry as it replaces PA at the surface, while PA impedes HCl entry as it replaces hexanol at the surface.

We can use eq 6 to predict f_{exch} for the mixture only at 0.02 M PA and 0.02 M hexanol, where both surface concentrations are known from the surface tension measurements. These values, obtained from interpolation in Figure 6c,d, are $c_{surf}^{hex} = 1.8 \times 10^{14}$ cm^{-2} and $c_{surf}^{PA} = 0.61 \times 10^{14}$ cm^{-2}, corresponding to surface mole fractions $x_{surf}^{hex} = 0.75$ and $x_{surf}^{PA} = 0.25$. The sum of these surface concentrations, $c_{surf}^{tot} = 2.4 \times 10^{14}$ cm^{-2}, is within 5% of the mole-fraction weighted average of PA and hexanol each at 0.04 M (the total surfactant concentration). This agreement implies that there are no strong interactions between the PA and hexanol molecules that significantly expand or contract the monolayer.

The form of eq 6 depends on the structure of the two-component film,[1,19] as discussed by Bertram and co-workers for N_2O_5 uptake through insoluble films on sulfuric acid.[18] When PA and hexanol mix completely and the HCl molecules interact statistically and independently with the chains and headgroups, eq 6 becomes

$$f_{exch}(\text{mixture}) = \left[1 - \langle a\rangle \frac{c_{surf}^{tot}}{c_{max}}\right]\left[f_{exch}(\text{bare}) + \langle b\rangle \frac{c_{surf}^{tot}}{c_{max}}\right] \quad (7a)$$

where $\langle a\rangle = a_{PA}x_{surf}^{PA} + a_{hex}x_{surf}^{hex}$ and $\langle b\rangle = b_{PA}x_{surf}^{PA} + b_{hex}x_{surf}^{hex}$ are mole-fraction weighted averages indicative of ideal mixing. If HCl instead diffuses through separate, immiscible domains of PA and hexanol molecules,[1,18,23] then eq 5 would be

$$f_{exch}(\text{mixture}) = \left[1 - a_{PA}\frac{c_{surf}^{tot}}{c_{max}}\right]\left[f_{exch}(\text{bare}) + b_{PA}\frac{c_{surf}^{tot}}{c_{max}}\right]x_{surf}^{PA} + \left[1 - a_{hex}\frac{c_{surf}^{tot}}{c_{max}}\right]\left[f_{exch}(\text{bare}) + b_{hex}\frac{c_{surf}^{tot}}{c_{max}}\right]x_{surf}^{hex} \quad (7b)$$

where we assume that the PA and hexanol domains have equal surface concentrations given by c_{surf}^{tot}.[65] With the values of a and b obtained from the fits in the top two panels of Figure 8, eqs 7a and 7b predict f_{exch} to be 0.138 and 0.141, in comparison with a measured value of 0.155 for the mixture. The predicted and measured values are close, but the overlap of the two predictions implies that H → D exchange measurements cannot be used to discriminate between miscible and immiscible films of PA and hexanol.

To test the model further, we extend this analysis to predict the HCl entry probability for *any* mixture of PA and hexanol in a two-step procedure. First, the two-component Langmuir model, eq 5, is used to estimate the partial surface concentrations c_{surf}^{PA} and c_{surf}^{hex} for a selected bulk-phase mixture of PA and hexanol. These values are then used to predict f_{exch} via eqs 7a or b. We apply this analysis to the data in Figure 8c for PA in 0.02 M hexanol and for hexanol in 0.02 M PA. The dashed-line fits correspond to eq 7a and show modest agreement with the measurements, differing at most by 0.04 in comparison with a total range of 0.09. We find that eqs 7a and 7b predict very similar values over the entire concentration range, precluding a choice between miscible and immiscible arrangements of the surface hexanol and PA molecules. This similarity and the modest agreement in Figure 8c, however, provides hope that models such as eqs 5 and 7, using data for individual surfactants, can potentially predict HCl entry probabilities over a wide range of surfactant concentrations in multicomponent mixtures.

Conclusions

The combined surface tension, Ar scattering, and HCl → DCl exchange measurements show that pentanoic acid can enhance HCl entry into cold sulfuric acid at low surface concentrations while impeding HCl entry as the hydrocarbon chains pack more tightly. In analogy with the OH groups of butanol and hexanol, the COOH group of pentanoic acid most likely provides extra protonation sites at the surface that catalyze HCl dissociation, followed by diffusion of Cl^- and H^+/D^+ into solution. A two-

step model in which HCl moves between the chains and then interacts with the headgroups reveals that PA is less effective than hexanol in dissociating HCl, as expected from its weaker basicity, and is also more compact than hexanol, perhaps because it forms dense, impermeable clusters or islands. The greater surface activity of hexanol makes the two-component mixture behave like pure hexanol unless PA is in great excess. These observations imply that even mixtures of short-chain alcohols and carboxylic acids can enhance HCl entry into sulfuric acid aerosols under stratospheric conditions, a conjecture we hope to explore further using different chain lengths and headgroups over a range of temperatures.

Acknowledgment. We thank the Air Force Office of Scientific Research for funding this research. We are also grateful to Collin Stecker and Betsy Solom for recording surface tensions and to Professor George Zografi for loan of a surface tensiometer.

References and Notes

(1) Gaines, G. L. *Insoluble Monolayers at Liquid-Gas Interfaces*; Interscience: New York, 1966.

(2) Donaldson, D. J.; Vaida, V. *Chem. Rev.* **2006**, *106*, 1445.

(3) Park, S.-C.; Burden, D. K.; Nathanson, G. M. *Acc. Chem. Res.* **2009**, *42*, 379.

(4) Gill, P. S.; Graedel, T. E.; Weschler, C. J. *Rev. Geophys. Space Phys.* **1983**, *21*, 903.

(5) Gilman, J. B.; Tervahattu, H.; Vaida, V. *Atmos. Environ.* **2006**, *40*, 6606.

(6) Murphy, D. M.; Thomson, D. S.; Mahoney, T. M. J. *Science* **1998**, *282*, 1664.

(7) Murphy, D. M.; Cziczo, D. J.; Hudson, P. K.; Thomson, D. S. *J. Geophys. Res. Atmos.* **2007**, *112*, D04203.

(8) Singh, H.; Chen, Y.; Staudt, A.; Jacob, D.; Blake, D.; Heikes, B.; Snow, J. *Nature* **2001**, *410*, 1078.

(9) Hanson, D. R.; Lovejoy, E. R. *J. Phys. Chem.* **1996**, *100*, 6397.

(10) Solomon, S. *Rev. Geophys.* **1999**, *37*, 275.

(11) Davidovits, P.; Kolb, C. E.; Williams, L. R.; Jayne, J. T.; Worsnop, D. R. *Chem. Rev.* **2006**, *106*, 1323.

(12) Fahey, D. W.; Kawa, S. R.; Woodbridge, E. L.; Tin, P.; Wilson, J. C.; Jonsson, H. H.; Dye, J. E.; Baumgardner, D.; Borrmann, S.; Toohey, D. W.; Avallone, L. M.; Proffitt, M. H.; Margitan, J.; Loewenstein, M.; Podolske, J. R.; Salawitch, R. J.; Wofsy, S. C.; Ko, M. K. W.; Anderson, D. E.; Schoeberl, M. R.; Chan, K. R. *Nature* **1993**, *363*, 509.

(13) Brown, S. S.; Ryerson, T. B.; Wollny, A. G.; Brock, C. A.; Peltier, R.; Sullivan, A. P.; Weber, R. J.; Dube, W. P.; Trainer, M.; Meagher, J. F.; Fehsenfeld, F. C.; Ravishankara, A. R. *Science* **2006**, *311*, 67.

(14) Thornton, J. A.; Braban, C. F.; Abbatt, J. P. D. N_2O_5 Hydrolysis on Sub-Micron Organic Aerosols. In. *Phys. Chem. Chem. Phys.* **2003**, *5*, 4593.

(15) Badger, C. L.; Griffiths, P. T.; George, I.; Abbatt, J. P. D.; Cox, R. A. *J. Phys. Chem. A* **2006**, *110*, 6986.

(16) McNeill, V. F.; Patterson, J.; Wolfe, G. M.; Thornton, J. A. *Atmos. Chem. Phys.* **2006**, *6*, 1635.

(17) Cosman, L. M.; Knopf, D. A.; Bertram, A. K. *J. Phys. Chem. A* **2008**, *112*, 2386.

(18) Cosman, L. M.; Bertram, A. K. *J. Phys. Chem. A* **2008**, *112*, 4625.

(19) Barnes, G. T. *Colloids Surf., A* **1997**, *126*, 149.

(20) Chuang, P. Y. *J. Geophys. Res.* **2003**, *108*, 4282.

(21) Zhang, J.; Unwin, P. R. *Langmuir* **2002**, *18*, 1218.

(22) Clifford, D.; Bartels-Rausch, T.; Donaldson, D. J. *Phys. Chem. Chem. Phys.* **2007**, *9*, 1362.

(23) Gilman, J. B.; Vaida, V. *J. Phys. Chem. A* **2006**, *110*, 7581.

(24) Borden, M. A.; Longo, M. L. *J. Phys. Chem. B* **2004**, *108*, 6009.

(25) For reviews of earlier studies, see refs 1, 2, 4, 42, and 55.

(26) Park, S.-C.; Burden, D. K.; Nathanson, G. M. *J. Phys. Chem. A* **2007**, *111*, 2921.

(27) Lawrence, J. R.; Glass, S. V.; Park, S.-C.; Nathanson, G. M. *J. Phys. Chem. A* **2005**, *109*, 7458.

(28) Glass, S. V.; Park, S.-C.; Nathanson, G. M. *J. Phys. Chem. A* **2006**, *110*, 7593.

(29) Morris, J. R.; Behr, P.; Antman, M. D.; Ringeisen, B. R.; Splan, J.; Nathanson, G. M. *J. Phys. Chem. A* **2000**, *104*, 6738.

(30) Klassen, J. K.; Hu, Z. J.; Williams, L. R. *J. Geophys. Res. Atmos.* **1998**, *103*, 16197.

(31) The diffusion depth z is calculated from $z_{rms} \approx 0.6\ (D\tau)^{1/2}$ for diffusion into the liquid over time $\tau/2$. For 68 wt % D_2SO_4 at 213 K, for example, $D \approx 5 \times 10^{-9}$ cm^2 s^{-1} and 200 μs, yielding $z_{rms} \approx 60$ Å. See also ref 26.

(32) Ardura, D.; Donaldson, D. J. *Phys. Chem. Chem. Phys.* **2009**, *11*, 857.

(33) Behr, P.; Morris, J. R.; Antman, M. D.; Ringeisen, B. R.; Splan, J. R.; Nathanson, G. M. *Geophys. Res. Lett.* **2001**, *28*, 1961.

(34) Torn, R. D.; Nathanson, G. M. *J. Phys. Chem. B* **2002**, *106*, 8064.

(35) Williams, L. R.; Long, F. S. *J. Phys. Chem.* **1995**, *99*, 3748.

(36) Klenø, J. G.; Kristiansen, M. W.; Nielsen, C. J.; Pedersen, E. J.; Williams, L. R.; Pedersen, T. *J. Phys. Chem. A* **2001**, *105*, 8440.

(37) Carslaw, K. S.; Clegg, S. L.; Brimblecombe, P. *J. Phys. Chem.* **1995**, *99*, 11557. M.Massucci, M.; Clegg, S. L.; Brimblecombe, P. *J. Phys. Chem. A* **1999**, *103*, 4209 Calculations from the aerosol inorganics model at http://mae.ucdavis.edu/wexler/aim.

(38) Lee, D. G.; Sadar, M. H. *Can. J. Chem.* **1976**, *54*, 3464.

(39) Lee, D. G.; Demchuk, K. J. *Can. J. Chem.* **1987**, *65*, 1769.

(40) Perdoncin, G.; Scorrano, G. *J. Am. Chem. Soc.* **1977**, *99*, 6983.

(41) Minerath, E. C.; Casale, M. T.; Elrod, M. J. *Environ. Sci. Technol.* **2008**, *42*, 4410.

(42) Lawrence, J. R.; Glass, S. V.; Nathanson, G. M. *J. Phys. Chem. A* **2005**, *109*, 7449.

(43) Defay, R.; Prigogine, I. *Surface Tension and Adsorption*; Wiley: New York, 1966; Chapter 2.

(44) Donaldson, D. J.; Anderson, D. *J. Phys. Chem. A* **1999**, *103*, 871.

(45) Equation 1 assumes constant activity coefficients over the 0−0.2 M addition of PA, We verified this assumption at 213 K by showing that the pentanoic acid evaporation signal is linear with bulk PA concentration up to 0.2 M. The evaporation signal is well fit by a Maxwell−Boltzmann distribution at 213 K at each concentration. These observations also imply that there is no barrier to PA evaporation itself by the PA film.

(46) For monolayer segregation, $\Gamma \approx c_{surf} + n^{2D}(1-\Gamma A_{surfactant})$, where $A_{surfactant} \approx 2 \times 10^{-15}$ cm^2 is the surface area of the surfactant molecule and n^{2D} is the monolayer concentration of the surfactant that would be found in the absence of segregation. It is given by $n^{2D} \approx c_{surfactant}/(c_{water}A_{water} + c_{acid}A_{acid})$, where c refers to the bulk-phase concentration. For 0.2 M PA in 68 wt % D_2SO_4, $\Gamma = 2.5 \times 10^{14}$ cm^{-2}, $c_{water} = 29$ M, $c_{acid} = 11.5$ M, $A_{water} = 10^{-15}$ cm^{-2}, $A_{acid} = 2 \times 10^{-15}$ cm^{-2}, we find that $n^{2D} = 4 \times 10^{12}$ cm^{-2} and $c_{surf} = 1.008\Gamma$. See also eq A.4 of: DeZwaan, J. L.; Brastad, S. M.; Nathanson, G. M. *J. Phys. Chem. C* **2007**, *112*, 3008.

(47) Myrick, S. H.; Franses, E. I. *Colloids Surf., A* **1998**, *143*, 503.

(48) Kralchevsky, P. A.; Danov, K. D.; Kolev, V. L.; Broze, G.; Mehreteab, A. *Langmuir* **2003**, *19*, 5004.

(49) Lunkenheimer, K.; Barzyk, W.; Hirte, R.; Rudert, R. *Langmuir* **2003**, *19*, 6140.

(50) The minimum surface area of normal C_3-C_{10} alcohols is given in ref 48 as 20.7 Å^2. The minimum surface area of normal carboxylic acids given in refs 49 and 51 is 22.6 Å^2 and is larger due to the greater size of COOH than OH. We use the one significant figure value of 20 Å^2 (or 5×10^{14} cm^{-2}) as a reference state for both hexanol and pentanoic acid in order to use a single gauge of the maximum possible chain−chain packing.

(51) Danov, K. D.; Kralchevsky, P. A.; Ananthapadmanabhan, K. P.; Lips, A. *J. Colloid Interface Sci.* **2006**, *300*, 809.

(52) Rubel, G. O. *J. Phys. Chem.* **1987**, *91*, 2103.

(53) When the acid is exposed to HCl for a time t_{exp}, the fraction of HCl molecules remaining in solution as HCl/Cl$^-$ is given by the time average of the uptake coefficient $\gamma(t)$, where $\langle\gamma(t_{exp})\rangle = (1/t_{exp})\int_0^{t_{exp}}\gamma(t)\ dt = \alpha(\tau/t_{exp})[\mathrm{erfc}(t_{exp}/\tau)^{1/2}e^{t/\tau} + (2/\pi)^{1/2}(t_{exp}/\tau)^{1/2} - 1]$. For $\tau = 130$ μs, $t_{exp} = 0.27$ s, and $\alpha = 0.46$, the equation predicts $\langle\gamma\rangle = 0.011$. See: Robinson, G. N.; Worsnop, D. R.; Jayne, J. T.; Kolb, C. E.; Swartz, E.; Davidovits, P. *J. Geophys. Res. Atmos.* **1998**, *103*, 25371.

(54) In refs 27 and 28, f_{exch} values for bare 60 and 68 wt % D_2SO_4 were reported as 0.52 ± 0.015 (eight measurements) and 0.15 ± 0.01 (three measurements), respectively. Our current experiments consistently yield 0.46 ± 0.01 (eight measurements) and 0.083 ± 0.002 (nine measurements). We have not been able to discover the source of this discrepancy. Fortunately, all interpretations of our data reflect only trends in f_{exch} upon addition of surfactant. These trends were reproduced for the addition of hexanol to 60 and 68 wt % D_2SO_4, and the shift seen in the pure f_{exch} values was found to be uniform for all surfactant concentrations.

(55) *Retardation of Evaporation by Monolayers: Transport Processes*; La Mer, V. K., Ed.; Academic Press: New York, 1962.

(56) Voss, L. F.; Hadad, C. M.; Allen, H. C. *J. Phys. Chem B* **2006**, *110*, 19487.

(57) Rychlicka-Rybska, J. *Colloid Surf., A* **1994**, *83*, 151.

(58) Dynaorwicz, P.; Paluch, M.; Rychlicka, J. *Colloid Polym. Sci.* **1989**, *267*, 451.

(59) We note that eq 6 generates an identical fit for negative values of a and b, namely, $a' = -b/f_{exch}$(bare) and $b' = -af_{exch}$(bare). In this picture, the alkyl chains enhance entry and the headgroups impede it. This scenario might apply to (1) polarizable gas molecules that dissolve well in the hydrocarbon chains and (2) headgroups that bind strongly to water, reducing the effective number of interfacial protonation sites. We do not believe

that this situation pertains to HCl because HCl entry through butanol and hexanol films at the same surface concentration is significantly lower for hexanol than for butanol. This comparison implies that, at fixed headgroup concentration, longer chains reduce HCl entry, in accord with a model in which the chains impede HCl transport. We also note that the second term in eq 6 may also be expressed as $f_{exch}(\text{bare})[1 - c_{surf}/c_{max}] + b''c_{surf}/c_{max}$, which takes into account the loss of free acid surface as the surfactant molecules take up space. The trends among the b and b'' values remain the same.

(60) Krisch, M. J.; D'Auria, R.; Brown, M. A.; Tobias, D. J.; Hemminger, J. C.; Ammann, M.; Starr, D. E.; Bluhm, H. *J. Phys. Chem. C* **2007**, *111*, 13497.

(61) Bran, R.; Casson, B. D.; Bain, C. D. *Chem. Phys. Lett.* **1995**, *245*, 326.

(62) Casson, B. D.; Bain, C. D. *J. Am. Chem. Soc.* **1999**, *121*, 2615.

(63) Vysotsky, Y. B.; Muratov, D. V.; Boldyreva, F. L.; Fainerman, V. B.; Vollhardt, D.; Miller, R. *J. Phys. Chem. B* **2006**, *110*, 4717.

(64) Vysotsky, Y. B.; Bryantsev, V. S.; Fainerman, V. B.; Vollhardt, D.; Miller, R. *J. Phys. Chem. B* **2002**, *106*, 121.

(65) The immiscible domain model requires knowledge of the surface densities of hexanol and PA in each domain. This information is not available; we know only the number of hexanol and PA molecules over the total area but not the area fractions of the domains. To make progress, we assume that the surface densities are the same and thus equal to $c_{surf}(\text{total}) = 2.4 \times 10^{14}$ cm^{-2}.

(66) Cox, R. A.; Yates, K. *J. Am. Chem. Soc.* **1978**, *100*, 3861.

(67) Myhre, C. E. L.; Christensen, D. H.; Nicolaisen, F. M.; Nielsen, C. J. *J. Phys. Chem. A* **2003**, *107*, 1979.

JP9072119